Journal for ImmunoTherapy of Cancer

Dynamic modulation of claudin18.2 expression and remodeling of the tumor microenvironment in gastric cancer during chemo-immunotherapy

Sung Hee Lim,[1] Takeshi Kuwata,[2] Minae An ,[1] Jung Yong Hong,[1] Seung Tae Kim,[1] Yuki Matsubara,[3] Kohei Shitara ,[3] Jeeyun Lee [1]

To cite: Lim SH, Kuwata T, An M, *et al*. Dynamic modulation of claudin18.2 expression and remodeling of the tumor microenvironment in gastric cancer during chemo-immunotherapy. *Journal for ImmunoTherapy of Cancer* 2025;**13**:e012683. doi:10.1136/jitc-2025-012683

► Additional supplemental material is published online only. To view, please visit the journal online (https://doi.org/10.1136/jitc-2025-012683).

SHL, TK and MA contributed equally.

Accepted 03 September 2025

[1]Division of Hematology-Oncology, Department of Medicine, Samsung Medical Center, Seoul, The Republic of Korea
[2]Department of Pathology and Clinical Laboratories, National Cancer Center-Hospital East, Kashiwa, Chiba, Japan
[3]Department of Gastroenterology and Gastrointestinal Oncology, National Cancer Center-Hospital East, Kashiwa, Japan

Correspondence to
Dr Kohei Shitara;
kshitara@east.ncc.go.jp

Dr Jeeyun Lee;
jyunlee@skku.edu

ABSTRACT

Background Claudin 18.2 (CLDN18.2) is a tight junction protein retained in malignant transformation of gastric cancer (GC) and is a promising therapeutic target. Despite the clinical benefit of zolbetuximab in CLDN18.2-positive tumors, the dynamic expression of CLDN18.2 during chemoimmunotherapy and its implications in the tumor microenvironment (TME) remain poorly understood.

Methods In a prospective single-arm phase II trial, we evaluated serial tumor biopsies from patients with advanced GC receiving first-line chemotherapy (capecitabine/oxaliplatin) with sequential pembrolizumab. CLDN18.2 expression was assessed by immunohistochemistry, and integrated molecular analyses—including whole transcriptome, whole exome, and single-cell RNA sequencing—were performed to explore TME alterations and molecular correlates.

Results Among 57 patients, 40.4% were CLDN18.2-positive at baseline. CLDN18.2 positivity was associated with diffuse-type histology, higher programmed death-ligand 1 (PD-L1) combined positive scores, and an immune-inflamed, stroma-rich TME characterized by enhanced T cell infiltration, transforming growth factor-β signaling, and matrix remodeling. Gene set enrichment analyses revealed immune activation and stromal remodeling in CLDN18.2-positive tumors. Single-cell analysis showed increased regulatory T cells and galectin-3-CD44 signaling in CLDN18.2-positive tumors. After one cycle of chemotherapy, CLDN18.2 expression was lost in 40% of initially positive tumors, while 10% of initially negative tumors gained expression—particularly in fibrotic TMEs. Survival outcomes were not significantly different between CLDN18.2-positive and CLDN18.2-negative groups; however, patients negative for both CLDN18.2 and PD-L1 showed poorer prognosis.

Conclusions CLDN18.2 expression is dynamically regulated during chemoimmunotherapy and is associated with a distinct immunosuppressive and fibrotic TME. These findings highlight the importance of repeated biomarker assessment and suggest potential combinatorial therapeutic strategies targeting both epithelial and stromal compartments in GC.

Trial registration number NCT04249739.

WHAT IS ALREADY KNOWN ON THIS TOPIC

⇒ Claudin 18.2 (CLDN18.2) expression in gastric cancer is known to be highly heterogeneous, with significant spatial variation within tumors, discordant expression between primary and metastatic sites.

WHAT THIS STUDY ADDS

⇒ CLDN18.2 expression is dynamically regulated during sequential chemo-immunotherapy in advanced gastric cancer, with conversion observed in approximately 20%–24% of patients.

⇒ CLDN18.2-positive tumors exhibit a unique tumor microenvironment, enriched with immune cells but dominated by stromal/fibrotic remodeling and transforming growth factor-β-driven signaling.

⇒ Integrative bulk and single-cell transcriptomic analyses identified CD44-galectin-3 crosstalk as a potential immunosuppressive axis within CLDN18.2-positive tumors.

HOW THIS STUDY MIGHT AFFECT RESEARCH, PRACTICE OR POLICY

⇒ Bidirectional changes in CLDN18.2 status during treatment underscore the importance of serial biomarker monitoring and the need to explore its prognostic and therapeutic relevance.

⇒ Distinct tumor microenvironment phenotype of Claudin 18.2-positive gastric cancer may suggest a need for combination strategies targeting both the tumor and its microenvironment.

INTRODUCTION

With the introduction of immunotherapy, the treatment landscape for gastric cancer (GC) is changing rapidly. Currently, the first-line standard treatment of locally advanced unresectable or metastatic GC is fluoropyrimidine/platinum plus antiprogrammed death-1 (anti-PD-1) monoclonal antibody.[1–3] Even in human epidermal growth factor receptor 2 (HER2)-positive GC, which is found in 15%–20% of stage IV GC, the addition of pembrolizumab to trastuzumab and

chemotherapy has become a new first-line standard of care in patients with programmed death-ligand 1 (PD-L1) expression level of ≥1 in terms of combined positive score (CPS) based on the KEYNOTE-811 trial.[4]

Claudin 18 isoform 2 (CLDN18.2), a member of the claudin family, is an important component of tight junction proteins that regulates tissue permeability, paracellular transport, and signal transduction.[5] CLDN18.2 is predominantly present in stomach mucosa and is retained during malignant transformation. Moreover, it may become more exposed and accessible in malignant tissues with disruption of tight junctions, which may make CLDN18.2 an attractive target for cancer treatment.[6] The prevalence of CLDN18.2 positivity is reported to be 35%–40% in patients with GC/gastroesophageal junction cancer (GEJC)[7–10] and is associated with the diffuse type.[11]

Zolbetuximab is a chimeric monoclonal antibody that binds to CLDN18.2, a target antigen specific to cancer cells,[12] and was initially developed for GC or GEJC. Two phase III studies (SPOTLIGHT and GLOW) demonstrated that zolbetuximab plus standard chemotherapy significantly prolonged survival compared with standard chemotherapy alone for CLDN18.2-positive (moderate-to-strong expression in ≥75% of tumor cells) GC/GEJC.[9 10] Moreover, the development of chimeric antigen receptor (CAR) T cell therapy, bispecific antibodies, and antibody-drug conjugates (ADC) drugs targeting CLDN18.2 is continuously progressing,[13] and promising results with CLDN18.2-redirected CAR-T cell therapy have been reported in early phase trials.[14 15]

Recently, we explored the role of sequentially added PD-1 inhibitor in the altered tumor microenvironment (TME) related to cytotoxic chemotherapy in a prospective single-arm phase II sequential chemoimmunotherapy trial (ClinicalTrial.gov identifier: NCT04249739).[16 17] Using acquired repeated biopsy samples from this trial, we aimed to evaluate the changes in CLDN18.2 status after one cycle of the first-line chemotherapy and explore the unique TME features in CLDN18.2-positive GC.

MATERIALS AND METHODS

Patients

We performed a phase II trial of capecitabine/oxaliplatin/pembrolizumab combination as first-line treatment in GC as a single-institute study with preplanned biomarker analysis.[16 17] Briefly, endoscopic biopsy was performed at baseline and after one cycle of capecitabine plus oxaliplatin (FU1), followed by a follow-up biopsy after five cycles of combination therapy with capecitabine/oxaliplatin/pembrolizumab. In this study, we evaluated the dynamic change in CLDN18.2 expression after one cycle of capecitabine/oxaliplatin, as well as the association of clinicopathological features of CLDN18.2 expression with other biomarkers—including human epidermal growth factor receptor 2 (HER2), mismatch repair/microsatellite instability (MSI), Epstein-Barr virus (EBV), and PD-L1 CPS—in patients with GC/GEJC. All samples analyzed in this study were tissues from patients who participated in our phase II clinical trial.[16] In this phase II trial, patients with HER2-negative GC received first-line CAPOX (oxaliplatin/capecitabine) in cycle 1 and then with the addition of pembrolizumab from cycle 2. HER2-positive patients were treated with trastuzumab plus cisplatin/capecitabine (XP) in cycle 1 and then the addition of pembrolizumab subsequently until progression. All primary tissues were collected from the patients who had biopsies before cycle 1, before cycle 2 (follow-up 1 (FU1)), and before cycle 7 (follow-up 2 (FU2)). Tumor tissues were obtained from endoscopic site-mapping biopsies. As a supplement analysis, prognostic impact of CLDN18.2 and CPS was tested in the Japanese patients who were treated by first-line chemotherapy plus anti-PD-1 therapy and participated in the biomarker study (UMIN000019129).

CLDN18.2 IMMUNOHISTOCHEMISTRY

Formalin-fixed, paraffin-embedded tissues were cut into 4 µm sections, mounted on Fisherbrand Superfrost Plus Microscope Slides (Thermo Fisher Scientific), and then dried at 60°C for 1 hour. Immunohistochemistry (IHC) staining was carried out on a BenchMark ULTRA (Roche Diagnostics) using the anti-CDLN18 antibody (43-14A, Roche Diagnostics) with the OptiView DAB IHC Detection Kit and counterstained with hematoxylin according to the manufacturer's instructions. CLDN18 protein expression was determined under a microscope, and CLDN18.2 positivity was defined as ≥75% of tumor cells demonstrating moderate-to-strong membranous staining as used in SPOTLIGHT and GLOW studies.

PROGRAMMED DEATH-LIGAND 1 IMMUNOHISTOCHEMISTRY

Tissues were freshly cut into 4 µm sections, mounted on Fisherbrand Superfrost Plus

Microscope Slides (Thermo Fisher Scientific) and then dried at 60°C for 1 hour. IHC staining was carried out on a Dako Autostainer Link 48 system (Agilent Technologies) using the Dako

PD-L1 IHC 22C3 pharmDx Kit (Agilent Technologies), with the EnVision FLEX Visualization

System and counterstained with hematoxylin, according to the manufacturer's instructions. PD-L1 protein expression was determined using CPS, which was the number of PD-L1-stained cells (tumor cells, lymphocytes, and macrophages) divided by the total number of viable tumor cells and multiplied by 100. The specimen was considered to have PD-L1 expression if CPS ≥1.

Whole exome and whole transcriptome sequencing

Tumor DNA and RNA were isolated from QIAamp Mini Kit (Qiagen) and Genomic DNA was extracted from matched peripheral blood using QIAamp DNA Blood Kit (Qiagen). Exome libraries were prepared from 1 µg of genomic DNA using the Agilent SureSelect Target

Enrichment protocol with the Human All Exon V6 probe set. DNA quality and concentration were evaluated by agarose gel electrophoresis and PicoGreen assay. The DNA was fragmented to 150–200 bp with a Covaris LE220 ultrasonicator, end-repaired, ligated to Agilent adapters, and PCR-amplified. Library size and concentration were assessed using the Agilent TapeStation D1000 system. For exome capture, 250 ng of DNA library was hybridized with the SureSelect All Exon Capture Library at 65 °C for 24 hours, followed by purification and further amplification. Final libraries were validated and quantified, then pooled and clustered for sequencing on an Illumina platform. RNA-sequencing (RNA-seq) libraries were generated using the Illumina Stranded messenger (mRNA) Prep Ligation Kit, following the manufacturer's instructions. Total RNA was purified, and mRNA was enriched using poly-T oligo-attached magnetic beads. The mRNA was then fragmented and complementary DNA was synthesized. Following end repair and adapter ligation, the libraries were amplified by PCR to enrich for successfully ligated fragments and to generate sufficient material for sequencing. The final libraries were purified to remove adapter dimers and other contaminants, and their quality and concentration were assessed using electrophoretic methods and quantitative PCR-based quantification. The prepared libraries were then pooled and subjected to high-throughput paired-end sequencing on an Illumina Novaseq 6000 platform.

Single-cell RNA sequencing

Tumor and paired normal tissues were dissociated into single-cell suspensions using the gentle MACS Dissociator and a tumor-infiltrating lymphocyte kit (Miltenyi Biotec), following the manufacturer's instructions. Cells were cryopreserved in liquid nitrogen and maintained high viability (~90%) after thawing. For single-cell RNA sequencing (scRNA-seq), up to 8000 cells per sample were processed using the 10x Genomics Chromium. Libraries were prepared with the Chromium Next GEM Single Cell 5 Reagent kit and sequenced on an Illumina NovaSeq 6000, targeting about 50 000 reads per cell. Sequencing data were aligned to the GRCh38 reference genome using CellRanger (10x Genomics).

Whole-exome sequencing and whole-transcriptome sequencing data analysis

Whole-exome sequencing data were aligned to the GRCh37 human reference genome using BWA-MEM.[18] The Genome Analysis Toolkit (V.4.1.1.02) was used for preprocessing to create BAM files for analysis. The preprocessing comprised base recalibration, indel realignment, and duplicate marking. To determine TCGA molecular subtype in advanced GC, we defined a genomic instability by counting the number of chromosomes altered either by deletion or amplification per sample (median for each chromosome ≠ 2) after running FACETS.[19] For whole-transcriptome sequencing data analysis, we used STAR (V.2.6.1)[20] to match the annotated RNA sequence reads to the human reference genome (GRCh38) after annotating them using ENSEMBL (V.98). Using the parameters suggested in the GTEx project, we quantified gene expression as transcripts per million using RSEM (V.1.3.1).

Single-cell RNA-seq analysis

The single-cell RNA-seq data from all samples were merged in R V.4.1 using the Seurat package V.4.0.[21] Doublets were excluded using Scrublet.[22] In addition, cells exhibiting a high mitochondrial read fraction (>30%) and low-quality libraries (<400 genes) were excluded. After scaling and standardizing the data from each sample, principal component analysis was performed. Batch correction was conducted using Harmony.[23] To visualize uniform manifold approximation and projection plots, we employed Monocle3.[24]

Statistical analysis

All statistical analyses were conducted using R V.4.1.1 (The R Foundation for Statistical Computing, www.R-project.org). Pearson's $\chi 2^2$ test or Fisher's exact test was used to compare discrete data. Overall survival (OS) was defined as the time from treatment initiation to any cause of death. Data cut-off for survival analysis was set at February 26, 2024. Survival outcomes were estimated using the Kaplan-Meier method and compared using the log-rank test. All p values were two-sided, and results were determined to be significant at $p<0.05$. The relationship between variables was quantified using Spearman's correlation, and the coefficient of determination (R) was calculated to assess the strength and direction for correlation.

RESULTS

Patient characteristics

A total of 57 patients with CLDN18.2 expression staining in baseline tumor tissue were included in this study (table 1). The median age of enrolled patients was 57 years, 77% were male. There were 10 HER2-positive and three EBV-positive tumors. 49 patients (86%) had PD-L1-positive tumors, while PD-L1 positivity was defined as CPS ≥1%. Three patients in this study had MSI-high tumors. The frequency of CPS ≥5 was significantly higher in the CLDN18.2-positive group compared with the CLDN18.2-negative group (65.2% vs 26.5%, p=0.006).

Relationship between CLDN18.2 and other molecular biomarkers

Comprehensive molecular features, including molecular subtypes, HER2, and PD-L1 CPS according to CLDN18.2 expressions, are shown in figure 1A. Among 57 patients with baseline CLDN18.2 status, the prevalence of CLDN18.2-positive tumors was 40% in all regardless of HER-2 status (HER2-negative GC, n=23, HER2-positive GC, n=4). CLDN18.2 positivity was represented in two of three (66.7%) in EBV-positive tumors and in one of three

Table 1 Baseline characteristics

Number of patients		57
Age, median (range)		57 (21–75)
Sex	Male	44 (77.2%)
	Female	13 (22.8%)
HER2		
Positive		10 (17.5%)
Negative		47 (82.5%)
EBV ISH		
Positive		3 (5.3%)
Negative		54 (94.7%)
PD-L1		
CPS, mean (range)		11.9 (0–95)
PD-L1 positive		49 (86.0%)
PD-L1 negative		8 (14.0%)
Status of MSI (by IHC or NGS)		
MSS		54 (94.7%)
MSI-high		3 (5.3%)

CPS, combined positive score; EBV, Epstein-Barr virus; HER2, human epidermal growth factor receptor 2; IHC, immunohistochemistry; ISH, in situ hybridization; MSI, microsatellite instability; MSS, microsatellite stability; NGS, next-generation sequencing; PD-L1, programmed death-ligand 1.

(33.3%) in MSI tumors. Of the 23 CLDN18.2-positive patients, 21 (91.3%) had a positive PD-L1 CPS of 1 or higher. Among them, 15 patients (65.2%) had PD-L1 CPS 5 or higher and six (26.1%) showed weak expression of <5 of CPS score (figure 1B). Four patients with both HER2-positive and CLDN18.2-positive tumors also had PD-L1 expressions, with three of them showing PD-L1 CPS 5 or higher. There were three patients with EBV (+) GCs, two were CLDN18.2 positive, and all of them showed PD-L1 expression of CPS 5 or higher (figure 1B). Further analysis revealed that when PD-L1 scores were categorized by tumor proportion score and tumor-infiltrating lymphocytes (TIL) and observed comprehensively,CLDN18.2-positive patients demonstrated higher scores of PD-L1 expression in immune cells as measured by TIL assessment (Mann-Whitney U test, p<0.05, online supplemental figure S1).

Transcriptomic analysis reveals CLDN18.2 association with immune activation and stromal remodeling in gastric cancer TME

To screen specific gene set enrichment in the overexpression of CLDN18.2 in tumor epithelial cells and their TME during their malignant transformation and disruption of cell polarity, we performed gene set variation analysis[25] in 40 patients who underwent whole transcriptomic sequencing simultaneously with CLDN18.2 IHC test. CLDN18.2 RNA was dominantly expressed in patients with advanced GC rather than CLDN18 isotype 1 RNA (online supplemental figure S2A) and positively correlated with CLDN18.2 IHC scores (Pearson's correlation, p<0.001, online supplemental figure S2B). As anticipated, CLDN18.2 RNA levels in CLDN18.2-positive groups (n=13) increased compared with CLDN18.2-negative groups (n=27) (online supplemental figure S2C). Since the results for RNA and protein were concordant, we proceeded to perform further transcriptional analysis. RNA genes in several canonical pathways showed distinctive patterns of enrichments between CLDN18.2-positive and CLDN18.2-negative samples. Notably, genes related to immune and inflammation pathways were significantly activated in CLDN18.2-positive groups (figure 2A). Moreover, gen sets representing the stroma-rich TME are highly enriched in CLDN18.2-positive groups. Tie2 expression is associated with angiogenesis and serves as a marker of aggressiveness in the hypoxic TME.[26] Transforming growth factor-β (TGF-β) signaling promotes epithelial-mesenchymal transition (EMT) and its activity is especially high in cancer-associated fibroblasts.[27] In particular, bone morphogenetic proteins, which are part of the TGF-β superfamily, are also active in the stroma-rich TME and contribute to tumor progression and stromal remodeling.[28] These signaling pathways are associated with diffuse type and poor prognosis and resistance to therapy. To clarify the differences in TME composition between CLDN18.2-positive and CLDN18.2-negative groups, we estimated four conserved TME subtypes—immune-depleted, fibrotic, immune-enriched, and immune-enriched/fibrotic—using the molecular functional portraits algorithm[29] based on whole transcriptomic expression data. Among the curated 29 functional gene expression signatures quantitatively reflecting the activity of key TME components, T cell traffic and matrix remodeling are significantly activated in CLDN18.2-positive groups compared with CLDN18.2-negative groups (Mann-Whitney U test, p<0.05, figure 2B). Subsequently, unsupervised clustering was performed to enable stratification of tumors into four TME. While fibrotic subtype was the most dominant population in CLDN18.2-positive groups, comprising 66.7%, it accounted for a smaller population in CLDN18.2-negative groups, at 33.3% (online supplemental figure S2C).

Disruption of cellular homeostasis and dysregulation of junctional protein

Through bulk transcriptomic analysis, we were able to screen signatures that are upregulated in the immune and stromal compartments of the TME in patients with CLDN18.2-positive GC. In addition, we identified several pathways that were downregulated on CLDN18.2 overexpression, and these pathways are involved in maintaining the structural integrity and homeostasis of epithelial cells. Acetylcholine is a major neurotransmitter that regulates epithelial barrier function and tight junction integrity in the gastrointestinal tract.[30] Calcium signaling is crucial for the regulation of tight junction assembly and epithelial barrier function.[31] Moreover, phospholipase-mediated

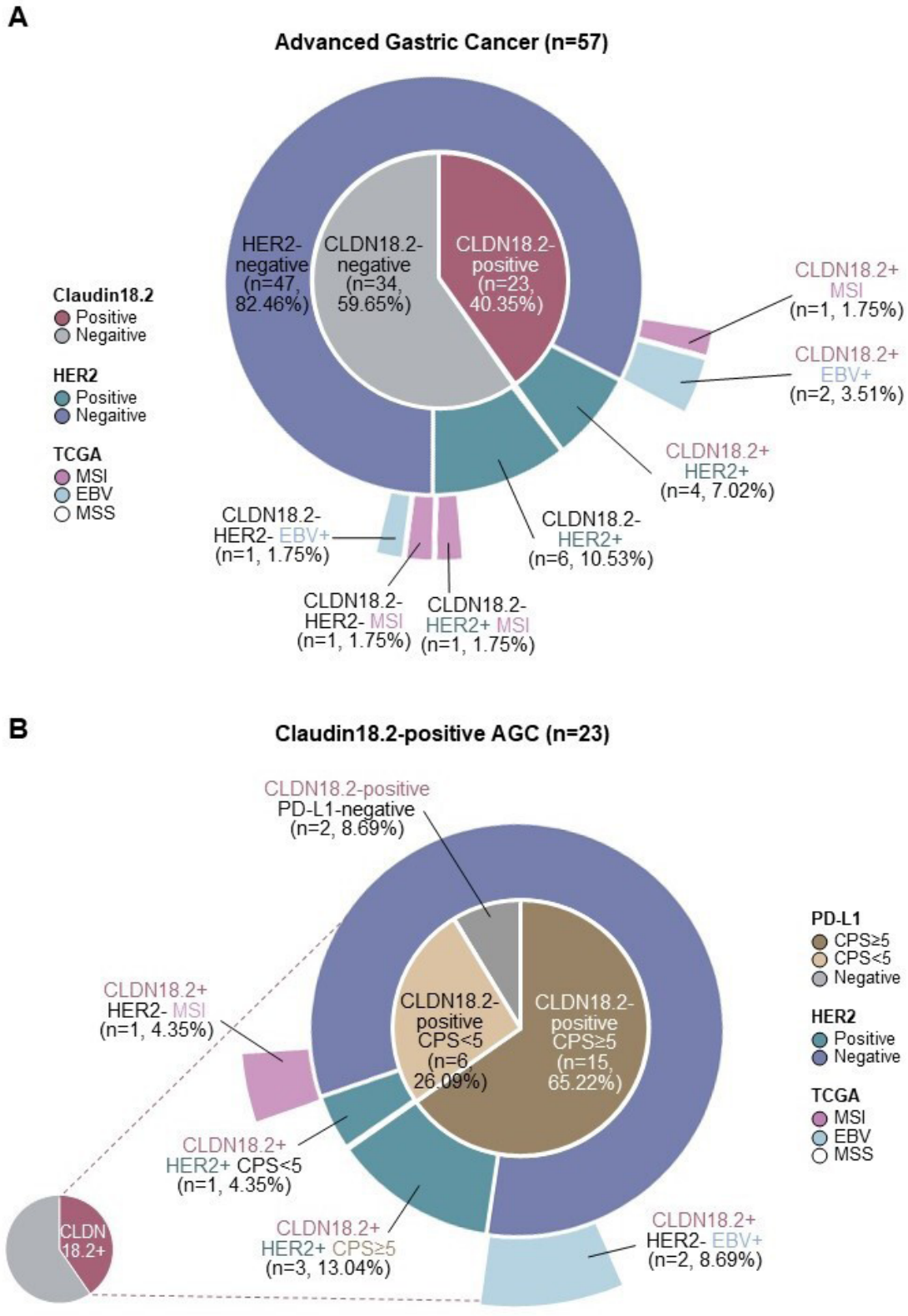

Figure 1 Relationship between CLDN18.2 and other molecular biomarkers. (A) CLDN18.2 and genetic characteristics in 57 patients with advanced gastric cancer. (B) CPS and genetic characteristics of the 23 CLDN18.2-positive patients. CLDN18.2, claudin18.2; CPS, combined positive score; TCGA, The Cancer Genome Atlas; HER2, human epidermal growth factor receptor 2; MSI, microsatellite instability; EBV, Epstein-Barr virus; MSS, microsatellite stability.

signaling cascades regulate the dynamics of tight junction proteins and epithelial cell adhesion[32] (figure 2A, bottom).

To clarify the dysregulation of tight junctions, we used scRNA-seq data including CLDN18.2-positive (n=11), CLDN18.2-negative (n=19), and their paired normal

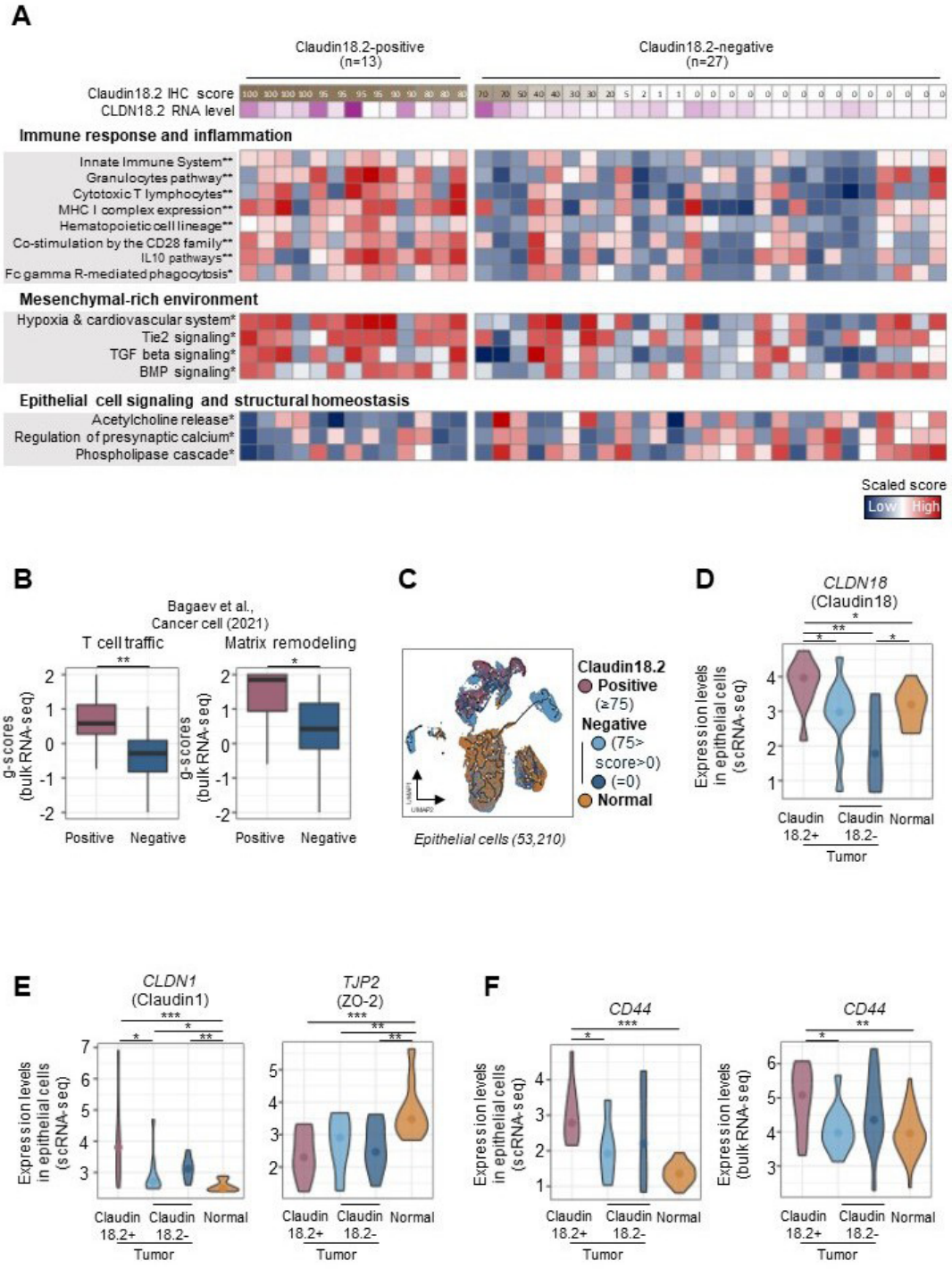

Figure 2 Association of CLDN18.2 expression with the transcriptomic reprogramming. (A) Heat maps of gene set variation analysis scores of different pathways between CLDN18.2-positive and CLDN18.2-negative groups. The top plot showing CLDN18.2 IHC scores and CLDN18.2 RNA expression levels. (B) Box plots showing different g-scores in T cell traffic and Matrix remodeling between CLDN18.2-positive and CLDN18.2-negative groups. (C) Uniform manifold approximation and projection embedding 53210 epithelial cells of scRNA-seq. CLDN18.2-positive tumor, two types of CLDN18.2-negative tumor, and normal epithelial cells were color-coded. (D) Violin plots depicting *CLDN18* expression levels across the CLDN18.2-positive tumor, CLDN18.2-negative tumor, and normal epithelial cells. (E) Violin plots showing heterogeneity of the representative tight junction gene levels across the CLDN18.2-positive tumor, CLDN18.2-negative tumor, and normal epithelial cells. (F) Cancer stem cell marker expression levels across CLDN18.2-positive tumors, CLDN18.2-negative tumors, and normal epithelial cells, as shown by violin plots of scRNA-seq and bulk RNA-seq data. BMP, bone morphogenetic protein; CLDN18.2, claudin 18.2; EBV, Epstein-Barr virus; HER2, human epidermal growth factor receptor 2; IHC, immunohistochemistry; IL, interleukin; MHC, major histocompatibility complex; MSS, microsatellite stability; MSI, microsatellite instability; scRNA-seq, single-cell RNA sequencing; TCGA, The Cancer Genome Atlas; TGF, transforming growth factor; ZO-2, zonula occludens-2. Statistical significance was determined by the Mann-Whitney U test. *P<0.05, **p<0.01, ***p<0.001.

data, when possible, to do normal tissue biopsies (n=20). Among 141 416 cells, we identified 53 210 epithelial cells and classified them into normal and tumor compartments by color-coding based on stratified CLDN18.2 IHC scores (figure 2C, online supplemental figure S3A and B). CLDN18 gene levels in tumors gradually increased and correlated with their stratification from a score of 0 to >75 based on CLDN18.2 IHC scores. Interestingly, CLDN18 expression in normal epithelial cells was upregulated compared with CLDN18.2-negative tumors with a score of 0 (figure 2D). CLDN1 expression was highly enriched in CLDN18.2-positive tumor cells compared with normal epithelial cells, whereas TJP2 (zonula occludens-2) was more abundant in normal epithelial cells than in CLDN18.2-positive tumor cells. We investigated the expression of other tight junction molecules and found that ACTB (actin) and TJP1 (zonula occludens-1) were aberrantly expressed compared with normal groups (figure 2E and online supplemental figure S2E and S3C). Differential gene expression analysis across tumor subgroups and normal cells revealed CD44 as significantly upregulated in Claudin18.2-positive tumor cells. CD44, a cancer stem cell marker linked to EMT, invasiveness, metastasis, and poor prognosis in gastric cancer, also correlates with immune infiltration. Consistent with scRNA-seq findings, bulk RNA-seq validation confirmed CD44 as a Claudin18.2-associated marker (figure 2F).

Distinct immune cell composition and galectin-3-CD44 crosstalk characterize claudin18.2-positive TME

Through scRNA-seq, we conducted cell type-specific transcriptomic profiling within this heterogeneous ecosystem, enabling precise dissection of molecular mechanisms underlying cellular crosstalk.[33] Our investigation focused on CLDN18.2-positive and CLDN18.2-negative subsets, employing stratified analysis of immune populations to reveal distinct interaction patterns between CLDN18.2-expressing malignant epithelial cells, tumor-associated macrophages and T cell subpopulations (figure 3A).

Globally, patients with CLDN18.2-positive tumors exhibited a statistically significant increase in both myeloid and T cell populations compared with CLDN18.2-negative patients (Mann-Whitney U test, p<0.05, figure 3B). Myeloid cells were further subdivided into four distinct (mast cells, dendritic cells, M1-like macrophage, and M2-like macrophage), among which M1-like macrophages and mast cells showed a significant but inverted pattern of difference between two groups (Mann-Whitney U test, p<0.05, figure 3C). Additionally, IL6 expression was elevated in total macrophages from CLDN18.2-positive tumors, suggesting that this inflammatory cytokine may act as a mediator linking CLDN18.2 overexpression in tumor cells to a disrupted epithelial barrier (Mann-Whitney U test, p<0.05, figure 3D).

We further subdivided T cells into CD4 (including regulatory T cells (Treg), helper T1/T17 cells, naïve and memory subsets), CD8 (naïve, memory, exhausted, and effector subsets), and a small proportion of mucosal-associated invariant T (MAIT) and γδT for detailed analysis. Although the difference was not statistically significant, CLDN18.2-positive group shows a higher median proportion of Tregs (CLDN18.2+, median=14.06 (range 7.69–44.76); CLDN18.2–, median=9.56 (range 2.88–23.15)) (figure 3E). Notably, we found that *LGALS3* (galectin-3), a molecule produced by TME, was significantly upregulated in CD4 T cells from CLDN18.2-positive tumors (Mann-Whitney U test, p<0.05) (figure 3F). This upregulation of galectin-3 was positively correlated with *CD44* expression on tumor cells, consistent with prior evidence that galectin-3 modulates *CD44* surface expression and function[34 35] (Spearman's correlation, r=0.649, p=0.04, figure 3G). While the best-known receptor-ligand interaction for *CD44* is with *LGALS9* (galectin-9), our data showed *LGALS9* expression correlated positively with *CD44* regardless of CLDN18.2 status (Spearman's correlation, r=0.413, p=0.029, figure 3H). Comprehensive analysis with CD44-galectin-3 crosstalk as a potential immunosuppressive TME is shown in online supplemental figure S4A. Exhausted CD8 T cell proportion was significantly higher in CLDN18.2+PD-L1 CPS ≥5 than CLDN18.2+PD-L1 CPS <5 (online supplemental figure S4B).

Changes in CLDN18.2 expression after chemo-immunotherapy

Of the total 57 patients with baseline CLDN18.2 status confirmed, there were 29 cases in which CLDN18.2 expression results were available at the baseline and FU1 by paired biopsy after one cycle of capecitabine/oxaliplatin chemotherapy. Among 10 patients with baseline CLDN18.2-positive, six retained CLDN18.2 expression after one cycle of chemotherapy, in four patients (40%), CLDN18.2 expression disappeared (figure 4A and C). In three patients (3/29, 10.3%) with no CLDN18.2 expression at baseline, the CLDN18 expression turned positive after one cycle of capecitabine plus oxaliplatin (XELOX) chemotherapy. Of note, all three patients with CLDN18.2 conversion after chemotherapy had poorly cohesive carcinoma. Moreover, their TME, as estimated by transcriptome data, was ultimately remodeled toward the fibrotic (F) subtype during chemoimmunotherapy (figure 4F). This observation suggests that the fibrotic enrichment of the TME, driven by mechanisms such as matrix remodeling, is closely associated with the transition of CLDN18.2 expression.

There were 10 patients whose CLDN18.2 status was available in the FU2 biopsy sample matched to baseline biopsy after adding six cycles of pembrolizumab to capecitabine/oxaliplatin. Figure 4B and D depicted dynamic expression of CLDN18.2 during chemo-immunotherapy. In six patients (6/10, 60%), the absence of CLDN18.2 expression at FU1 was maintained at FU2 and two patients (2/10, 20%) continued to have CLDN18.2 expression in their tumor after the addition of pembrolizumab. Among the 10 patients with a complete set of three paired biopsy results, nine were PD-L1 positive at baseline, and their PD-L1 CPS values changed following

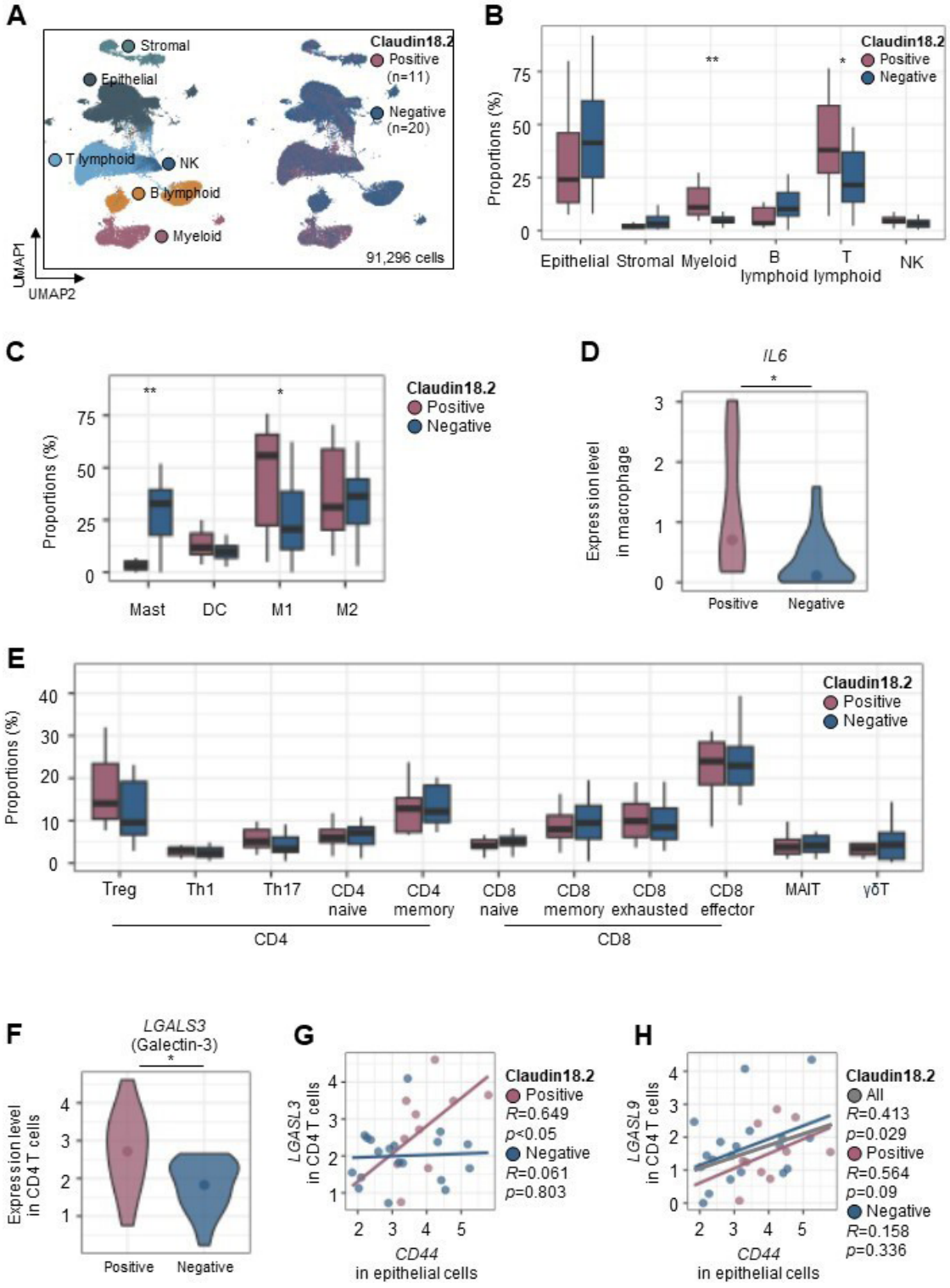

Figure 3 Association of CLDN18.2 expression with infiltration of immune cells. (A) UMAP embedding 91 296 total cells from tumor biopsy. CLDN18.2-positive, CLDN18.2-negative groups and six cell types were color-coded. (B) Comparing the tumor and microenvironment population between CLDN18.2-positive and CLDN18.2-negative tumors. (C) Comparing the myeloid subpopulation between CLDN18.2-positive and CLDN18.2-negative groups. (D) Violin plots showing different *IL6* expressions in macrophage between CLDN18.2-positive and CLDN18.2-negative tumors. (E) Comparing the T lymphoid subpopulation between CLDN18.2-positive and CLDN18.2-negative groups. (F) Violin plots showing different *LGALS3* expressions in CD4 T cells between CLDN18.2-positive and CLDN18.2-negative tumors. Statistical significance was determined by the Mann-Whitney U test. *P<0.05, **p<0.01. (G) Correlation analysis between LGALS3 and CD44 expressions. (H) Correlation analysis between LGALS3 and CD44 expressions. Relationship between two variables was quantified using Spearman's correlation. CLDN18.2, claudin 18.2; DC, dendritic cell; IL, interleukin; MAIT, mucosal-associated invariant T; NK, natural killer; Th, T helper; Treg, regulatory T cell; UMAP, uniform manifold approximation and projection.

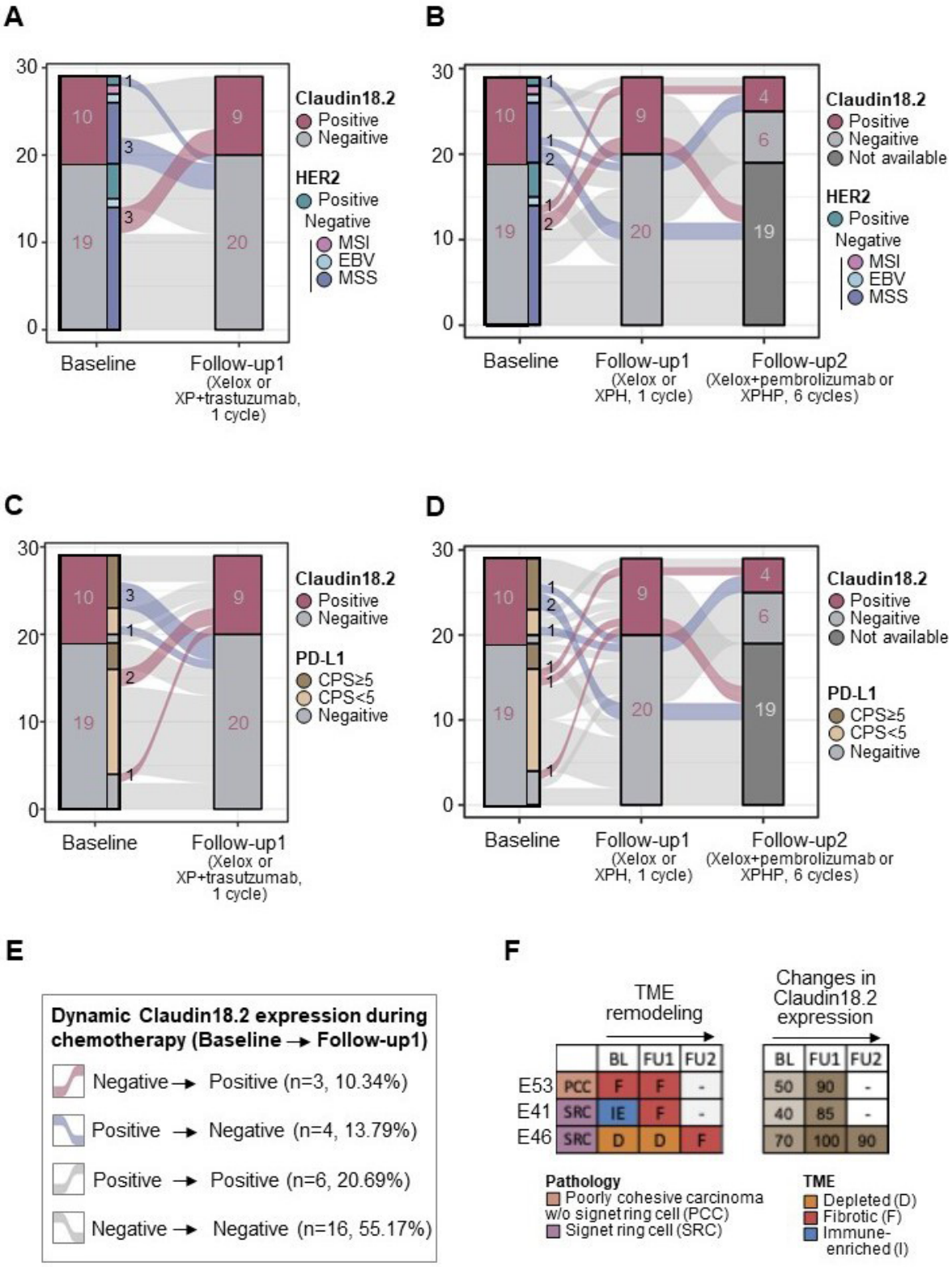

Figure 4 Dynamic expression of CLDN18.2 during chemo-immunotherapy**.** Paired samples with available results at the baseline and follow-up1 were 29 patients. (A, C) Sankey plot demonstrating a dynamic change of CLDN18.2 expression during chemotherapy. (B, D) Sankey plot demonstrating a dynamic change of CLDN18.2 expression during chemo-immunotherapy. (A, B) Samples are grouped by CLDN18.2, HER2, and genetic characteristics. (C, D) Each patient is colored by CLDN18.2 and PD-L1 CPS. (E) Overview of expression of CLDN18.2 across time points. (F) TME remodeling in CLDN18.2 transition group from negative to positive. CLDN18.2, cclaudin18.2; CPS, combined positive score; EBV, Epstein-Barr virus; HER2, human epidermal growth factor receptor 2; MSI, microsatellite instability; MSS, microsatellite stability; PD-L1, programmed death-ligand 1; TME, tumor microenvironment; XELOX, capecitabine plus oxaliplatin; XPH, capecitabine, cisplatin, and trastuzumab; XPHP, capecitabine, cisplatin, and trastuzumab with pembrolizumab.

chemo-immunotherapy. However, no significant relationship with change in CLDN18.2 expression was observed (figure 4D).

Figure 5 demonstrates the influence of chemotherapy on CLDN18.2 expression. Figure 5A shows the positive conversion of CLDN18.2 after one cycle of capecitabine/oxaliplatin. The CLDN18.2(+) GC changed to CLDN18.2(−) tumor after one cycle of chemotherapy as shown in figure 5B and figure 5C.

Survival outcomes

No significant OS was observed between the patients with baseline CLDN18.2-positive tumors and those with CLDN18.2-negative tumors (median 20.0 months (95% CI 15.0 to 25.0) vs 18.3 months (95% CI 7.9 to 26.3), p=0.939) (online supplemental figure S5). Kaplan-Meier curve was the result of analyzing the OS by dividing patients into several groups according to the level of PD-L1 expression and CLDN18.2 positivity (figure 6A). The OS for standard first-line treatment was poor in the patients without both CLDN18.2 and PD-L1 expression, although it was not statistically significant (figure 6B). We performed additional survival analyses by combining the survival data of 74 patients treated with first-line chemotherapy plus nivolumab or pembrolizumab at the National Cancer Center (Japan) (online supplemental figure S6). The baseline CLDN18.2 positivity did not show a significant difference in progression-free survival and OS in a total of 133 patients with GC treated with first-line chemotherapy+immunotherapy. The median OS of patient's double negative for both CLDN18.2 and PD-L1 was 12.7 months, which was numerically lower than that of the other groups, but the difference was not significant.

DISCUSSION

Our study demonstrates that CLDN18.2 expression is dynamically regulated in GC and can be modulated in response to sequential chemo-immunotherapy. Following a single cycle of chemotherapy, 40% of tumors with baseline CLDN18.2 positivity lost detectable expression, while approximately 10% of initially CLDN18.2-negative tumors gained expression. Importantly, this positive conversion was accompanied by marked stromal remodeling, with the TME shifting toward a fibrotic phenotype enriched in extracellular matrix components. These findings suggest that CLDN18.2 is not a fixed biomarker, but one that evolves with treatment, reinforcing the need for serial assessment to guide therapeutic decision-making and stratify patients for CLDN18.2-targeted therapies. Baseline analyses revealed that CLDN18.2-positive GCs harbor distinctive TME features. These tumors frequently exhibited an immune-infiltrated phenotype, with 65.2% of CLDN18.2-positive cases demonstrating PD-L1 CPS ≥5, significantly higher than in CLDN18.2-negative tumors (26.5%, p=0.006). Notably, PD-L1 expression was enriched on tumor-infiltrating immune cells in the CLDN18.2-positive subgroup. This observation aligns with recent reports highlighting the presence of natural killer cells—particularly in EBV-positive, CLDN18.2-expressing tumors—which may contribute to antibody-dependent cellular cytotoxicity.[36] Transcriptomic profiling further supported this immune-active landscape, revealing upregulation of immune-related and inflammation-related gene pathways in CLDN18.2-positive tumors compared with negatives. These findings suggest that CLDN18.2-positive patients may benefit from combinatorial strategies involving anti-CLDN18.2 agents and immune checkpoint inhibitors, potentially contributing to improved clinical outcomes in this biomarker-defined subgroup.[37]

At the same time, gene sets associated with stromal and fibrotic pathways, including angiogenesis via Tie2 and TGF-β/BMP signaling, were significantly enriched in CLDN18.2-positive tumors, underscoring the desmoplastic and stromal-rich nature of diffuse-type GCs. Based on established TME classifications, the majority of CLDN18.2-positive tumors were categorized as 'fibrotic', marked by heightened extracellular matrix remodeling and TGF-β pathway activation. This integrated transcriptomic and immunological profile suggests a TME characterized by both immune cell infiltration and a stromal barrier, a configuration commonly associated with resistance to immune checkpoint blockade. scRNA-seq provided high-resolution insights into the cellular composition and intercellular interactions within CLDN18.2-positive TMEs. Among malignant epithelial cells, CD44 emerged as one of the top differentially expressed genes associated with CLDN18.2 positivity. CD44, a well-established marker of cancer stemness and EMT in GC, is implicated in tumor invasiveness, metastasis, and therapeutic resistance.[38] Beyond its prognostic value, CD44 expression has been linked to the degree of immune infiltration in GC.[39] Immune profiling at the single-cell level revealed that CLDN18.2-positive tumors harbored significantly higher proportions of both myeloid and T cell populations compared with CLDN18.2-negative tumors. M1-like macrophages in CLDN18.2-positive tumors expressed elevated levels of interleukin-6 (IL-6), a pro-inflammatory cytokine known to disrupt epithelial junction integrity and drive tumor progression. Consistent with prior findings from multiplex IHC studies showing increased $CD8^+$ and $CD4^+$ T cells and M1 macrophages in CLDN18.2-high tumors, we also observed immunologically active but potentially immunosuppressive TMEs.[40] Notably, galectin-3 (LGALS3) was significantly upregulated in $CD4^+$ T cells within CLDN18.2-positive tumors. Galectin-3 is an immunoregulatory lectin secreted by macrophages and other stromal components, known to suppress T cell effector functions and enhance tumor invasiveness. Importantly, galectin-3 expression in T cells strongly correlated with CD44 expression on tumor cells (Spearman's r=0.65), suggesting a galectin-3/CD44 axis as a potential mediator of tumor-immune cell crosstalk. Given galectin-3's ability to bind and cluster CD44 on the tumor surface, modulating downstream signaling, this interaction may contribute to immune resistance and

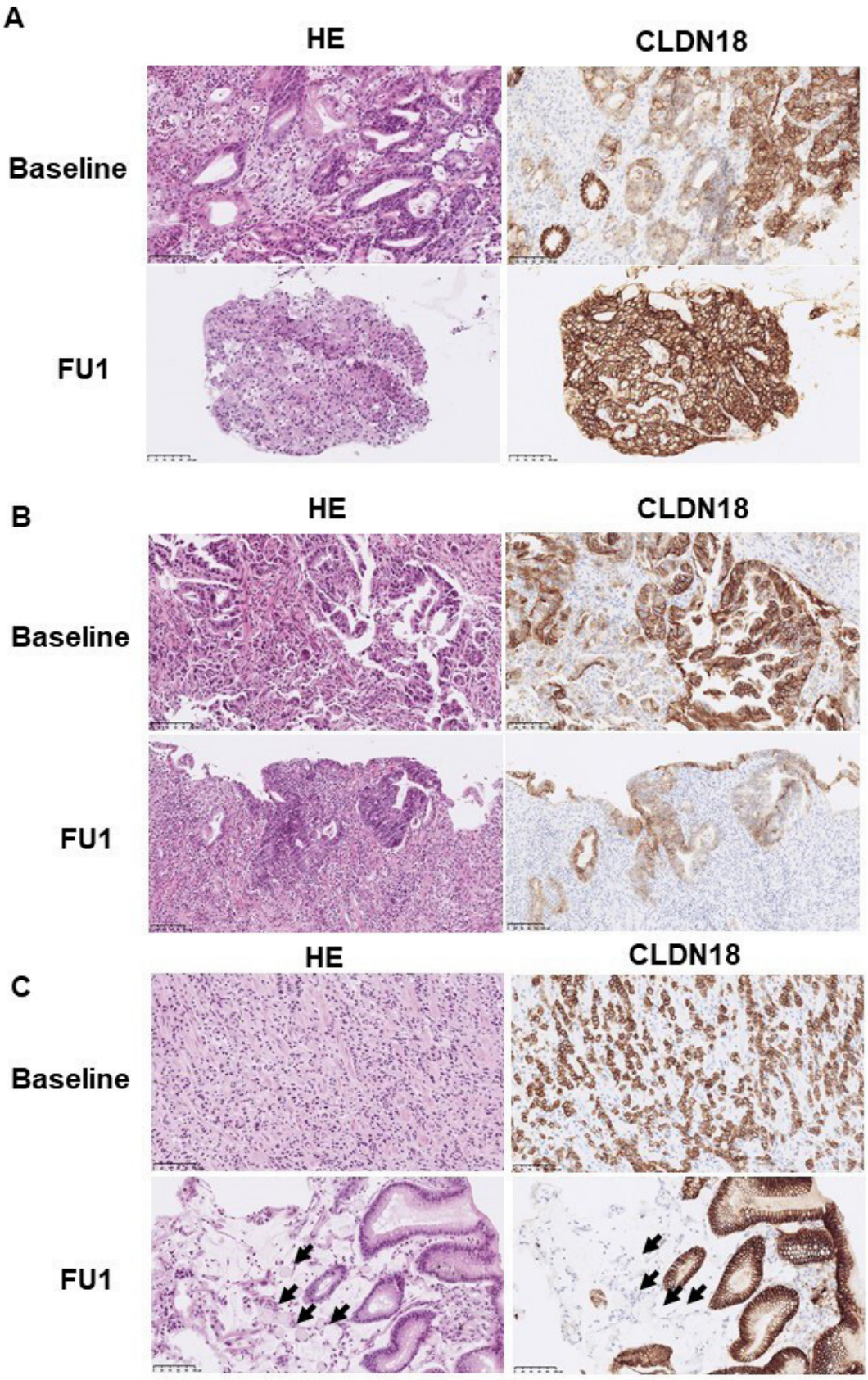

Figure 5 Influence of chemotherapy on CLDN18.2 expression. (A) Positive conversion of CLDN18.2 expression after chemotherapy. (B) Negative conversion of CLDN18.2 expression after chemotherapy. (C) CLDN18.2 expression between prechemotherapy and postchemotherapy. Negative conversion of CLDN18.2 expression after chemotherapy. Poorly cohesive carcinoma showed ubiquitous strong membranous staining in baseline, while membranous staining was lost in remaining signet ring cells (arrowed). CLDN18.2, claudin18.2; FU1, follow-up1.

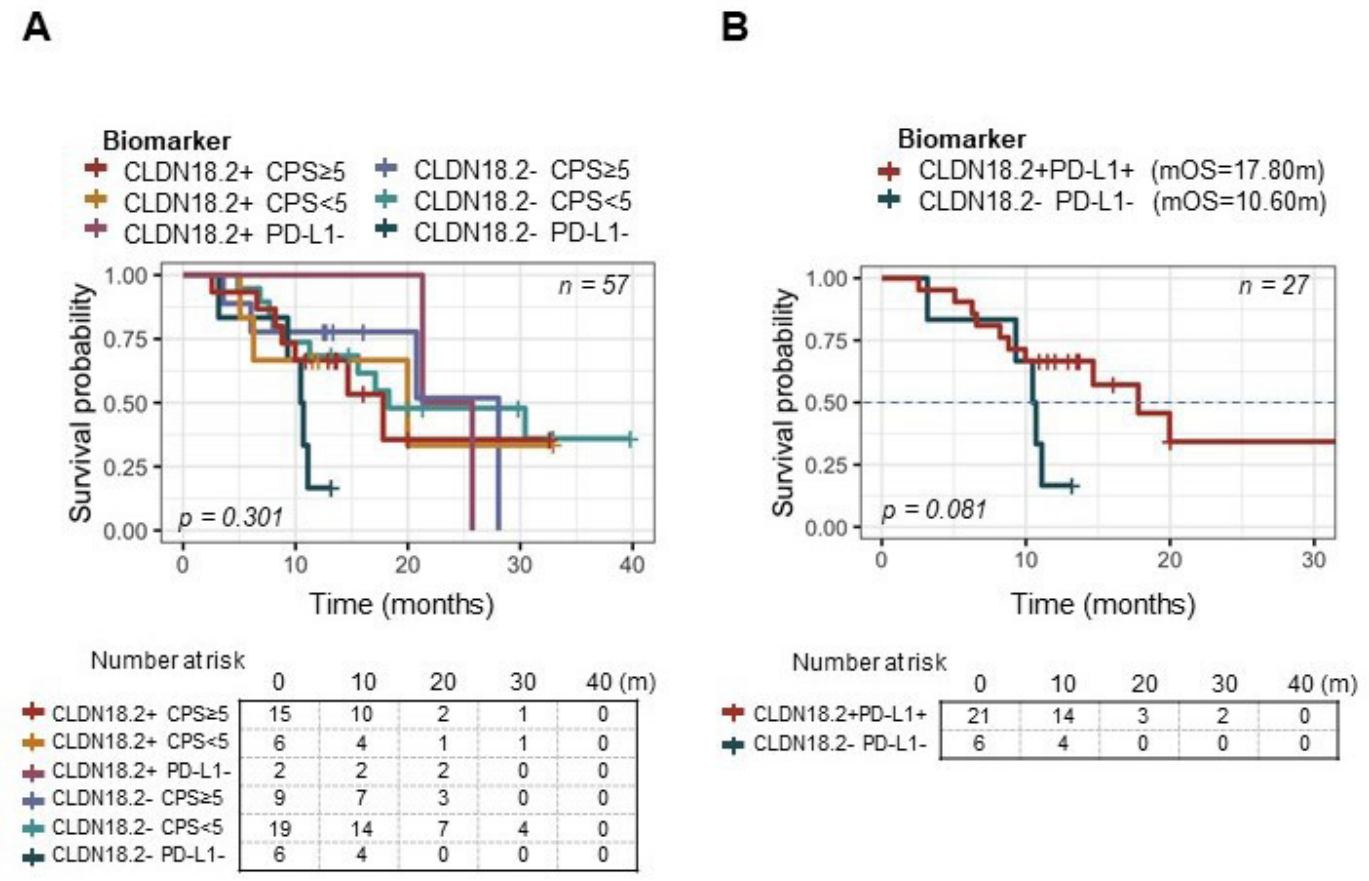

Figure 6 Kaplan-Meier curves of for each group according to CLDN18.2 and CPS. (A) Kaplan-Meier plot showing diverse OS probability of 57 patients with AGC according to heterogeneous biomarkers. (B) Kaplan-Meier plot demonstrating the difference in OS between CLDN18.2-positive/CPS ≥5 and CLDN18.2-negative/PD-L1-negative groups. Statistical comparison was performed using a log-rank test. AGC, advanced gastric cancer; CLDN18.2, claudin18.2; CPS, combined positive score; mOS, median OS; OS, overall survival; PD-L1, programmed death-ligand 1.

stromal remodeling. These findings propose galectin-3 as a rational combinatorial target alongside CLDN18.2-directed therapies.

The strength of our study lies in its design as a prospective phase II clinical trial with *preplanned serial biopsies*, enabling direct observation of *dynamic changes in CLDN18.2 expression* over time. By obtaining repeated biopsies from the same tumor sites before and after chemotherapy alone and again following the addition of anti-PD-1 therapy, we were able to capture temporal and treatment-related alterations in the TME. Furthermore, the assessment of CLDN18.2 expression was conducted using criteria consistent with those employed in pivotal zolbetuximab trials, thereby enhancing the *clinical relevance and reproducibility* of our findings.

In our study, 23 of 57 patients (40.3%) with assessable baseline tumor samples were classified as CLDN18.2-positive, a frequency highly consistent with the 38.4% positivity rates reported in both the GLOW and SPOTLIGHT trials.[9 10] CLDN18.2 expression was further analyzed in relation to other biomarkers. Among patients with HER2-positive GC, the CLDN18.2 expression rate was similar to that of the overall cohort. In contrast, CLDN18.2 expression was elevated to 67% in EBV-positive tumors, echoing prior reports of higher CLDN18.2 expression in EBV-associated GC subtypes.[36 41] Four patients (7.0%) in our study exhibited co-expression of HER2 and CLDN18.2, a slightly higher frequency than previously reported co-expression rates of approximately 4%–5%.[42 43] These findings reinforce the potential of CLDN18.2 as a complementary therapeutic target alongside HER2, warranting further investigation into the treatment implications for this biomarker-defined subgroup.

Following one cycle of chemotherapy (XELOX or XP+trastuzumab), *CLDN18.2 expression remained stable in 22 of 29 patients (76%)*, a concordance rate consistent with prior studies.[43] However, 14% of patients exhibited loss of CLDN18.2 expression, while 10% demonstrated gain of CLDN18.2 positivity despite being negative at baseline. Although limited by sample size, transcriptomic analyses revealed that tumors converting from CLDN18.2-negative to CLDN18.2-positive displayed features of a fibrotic TME, suggesting that stromal remodeling may facilitate CLDN18.2 re-expression during treatment. There were no significant differences in OS between the

CLDN18.2-positive and CLDN 18.2-negative groups in this cohort, which aligns with previous studies.[43–45] Although the sample size was small, we observed that patients with metastatic GC lacking both CLDN18.2 and PD-L1 expression had a substantially unfavorable prognosis within our study cohort. Further validation in a larger cohort is needed to verify these findings.

A key limitation of this study is the relatively small sample size, with CLDN18.2 baseline expression assessable in 57 patients, and paired biopsies available for 29 patients, including triple paired samples in 10 cases. Despite this, the study provides valuable insight into the dynamic modulation of CLDN18.2 expression throughout the course of chemo-immunotherapy. While the changes in CLDN18.2 expression observed after a single treatment cycle may reflect treatment-induced modulation, the potential influence of intratumoral heterogeneity cannot be excluded.

In conclusion, CLDN18.2-positive GCs demonstrate a distinct TME characterized by a dual landscape of fibrosis and immune cell infiltration. This includes pro-inflammatory M1 macrophages and IL-6-mediated matrix remodeling, alongside immunosuppressive pathways involving CD44 and galectin-3, suggesting a complex interplay between immune activation and immune evasion. Using serial tumor biopsies, we observed temporal changes in CLDN18.2 expression in approximately 20%–24% of patients during treatment, underscoring the need for dynamic biomarker assessment and further mechanistic studies to guide optimized, biomarker-informed therapeutic strategies.

Contributors Conceptualization: JL; formal analysis: SHL, TK, MA; investigation: SHL, JYH, STK, JL, TK, YM, KS; writing—original draft: SHL, TK, MA; writing—review and editing: all authors. JL served as the guarantor. She accepts full responsibility for the integrity of the work as a whole, had access to the data, and controlled the decision to publish.

Funding This research was supported by the Bio & Medical Technology Development Program of the National Research Foundation (NRF), funded by the Korean government (MSIT) (No. RS-2023-00222838).

Competing interests KS reports receiving personal fees for consulting and advisory roles from Bristol Myers Squibb, Takeda, Ono Pharmaceutical, Novartis, Daiichi Sankyo, Amgen, Boehringer Ingelheim, Merck Pharmaceutical, Astellas, Guardant Health Japan, Janssen, AstraZeneca, Zymeworks Biopharmaceuticals, ALX Oncology, and Bayer; receiving honoraria from Bristol Myers Squibb, Ono Pharmaceutical, Janssen, Eli Lilly, Astellas, and AstraZeneca; and receiving research funding (all to institution) from Astellas, Ono Pharmaceutical, Daiichi Sankyo, Taiho Pharmaceutical, Chugai, Merck Pharmaceutical, Amgen, Eisai, PRA Health Sciences, and Syneos Health, outside the submitted work. JL reports advisory/consultation roles from Astellas, Amgen, AstraZeneca, Daiichi Sankyo, and Bristol Myers Squibb. The authors declare that they have no known competing financial interests or personal relationships that could have appeared to influence the work reported in this paper.

Patient consent for publication Not applicable.

Ethics approval The study was reviewed and approved by the Institutional Review Board (IRB) of Samsung Medical Center (Seoul, Korea; IRB No. 2019-11-089). The requirement for informed consent was waived owing to this study's retrospective nature.

Provenance and peer review Not commissioned; externally peer reviewed.

Data availability statement Data are available on reasonable request.

ORCID iDs
Minae An http://orcid.org/0009-0007-9575-7952
Kohei Shitara http://orcid.org/0000-0001-5196-3630
Jeeyun Lee http://orcid.org/0000-0002-4911-6165

REFERENCES

1 Janjigian YY, Shitara K, Moehler M, *et al*. First-line nivolumab plus chemotherapy versus chemotherapy alone for advanced gastric, gastro-oesophageal junction, and oesophageal adenocarcinoma (CheckMate 649): a randomised, open-label, phase 3 trial. *Lancet* 2021;398:27–40.
2 Rha SY, Oh D-Y, Yañez P, *et al*. Pembrolizumab plus chemotherapy versus placebo plus chemotherapy for HER2-negative advanced gastric cancer (KEYNOTE-859): a multicentre, randomised, double-blind, phase 3 trial. *Lancet Oncol* 2023;24:1181–95.
3 Xu R-H, Oh D-Y, Kato K, *et al*. LBA80 Tislelizumab (TIS) plus chemotherapy (Chemo) vs placebo (PBO) plus chemo as first-line (1L) treatment of advanced gastric or gastroesophageal junction adenocarcinoma (GC/GEJC): Final analysis results of the RATIONALE-305 study. *Ann Oncol* 2023;34:S1320–1.
4 Janjigian YY, Kawazoe A, Bai Y, *et al*. Pembrolizumab plus trastuzumab and chemotherapy for HER2-positive gastric or gastro-oesophageal junction adenocarcinoma: interim analyses from the phase 3 KEYNOTE-811 randomised placebo-controlled trial. *Lancet* 2023;402:2197–208.
5 Niimi T, Nagashima K, Ward JM, *et al*. claudin-18, a novel downstream target gene for the T/EBP/NKX2.1 homeodomain transcription factor, encodes lung- and stomach-specific isoforms through alternative splicing. *Mol Cell Biol* 2001;21:7380–90.
6 Sahin U, Koslowski M, Dhaene K, *et al*. Claudin-18 splice variant 2 is a pan-cancer target suitable for therapeutic antibody development. *Clin Cancer Res* 2008;14:7624–34.
7 Rohde C, Yamaguchi R, Mukhina S, *et al*. Comparison of Claudin 18.2 expression in primary tumors and lymph node metastases in Japanese patients with gastric adenocarcinoma. *Jpn J Clin Oncol* 2019;49:870–6.
8 Sahin U, Türeci Ö, Manikhas G, *et al*. FAST: a randomised phase II study of zolbetuximab (IMAB362) plus EOX versus EOX alone for first-line treatment of advanced CLDN18.2-positive gastric and gastro-oesophageal adenocarcinoma. *Ann Oncol* 2021;32:609–19.
9 Shah MA, Shitara K, Ajani JA, *et al*. Zolbetuximab plus CAPOX in CLDN18.2-positive gastric or gastroesophageal junction adenocarcinoma: the randomized, phase 3 GLOW trial. *Nat Med* 2023;29:2133–41.
10 Shitara K, Lordick F, Bang Y-J, *et al*. Zolbetuximab plus mFOLFOX6 in patients with CLDN18.2-positive, HER2-negative, untreated, locally advanced unresectable or metastatic gastric or gastro-oesophageal junction adenocarcinoma (SPOTLIGHT): a multicentre, randomised, double-blind, phase 3 trial. *Lancet* 2023;401:1655–68.
11 Pellino A, Brignola S, Riello E, *et al*. Association of CLDN18 Protein Expression with Clinicopathological Features and Prognosis in Advanced Gastric and Gastroesophageal Junction Adenocarcinomas. *J Pers Med* 2021;11:1095.
12 Sahin U, Schuler M, Richly H, *et al*. A phase I dose-escalation study of IMAB362 (Zolbetuximab) in patients with advanced gastric and gastro-oesophageal junction cancer. *Eur J Cancer* 2018;100:17–26.
13 Nakayama I, Qi C, Chen Y, *et al*. Claudin 18.2 as a novel therapeutic target. *Nat Rev Clin Oncol* 2024;21:354–69.
14 Botta GP, Chao J, Ma H, *et al*. Metastatic gastric cancer target lesion complete response with Claudin18.2-CAR T cells. *J Immunother Cancer* 2024;12:e007927.

15 Qi C, Gong J, Li J, *et al*. Claudin18.2-specific CAR T cells in gastrointestinal cancers: phase 1 trial interim results. *Nat Med* 2022;28:1189–98.
16 An M, Mehta A, Min BH, *et al*. Early immune remodeling steers clinical response to frontline chemoimmunotherapy in advanced gastric cancer. *Cancer Discov* 2024.
17 Lim SH, An M, Lee H, *et al*. Determinants of Response to Sequential Pembrolizumab with Trastuzumab plus Platinum/5-FU in HER2-Positive Gastric Cancer: A Phase II Chemoimmunotherapy Trial. *Clin Cancer Res* 2025;31:1476–90.
18 Li H, Durbin R. Fast and accurate short read alignment with Burrows-Wheeler transform. *Bioinformatics* 2009;25:1754–60.
19 Shen R, Seshan VE. FACETS: allele-specific copy number and clonal heterogeneity analysis tool for high-throughput DNA sequencing. *Nucleic Acids Res* 2016;44:e131.
20 Dobin A, Davis CA, Schlesinger F, *et al*. STAR: ultrafast universal RNA-seq aligner. *Bioinformatics* 2013;29:15–21.
21 Stuart T, Butler A, Hoffman P, *et al*. Comprehensive Integration of Single-Cell Data. *Cell* 2019;177:1888–902.
22 Wolock SL, Lopez R, Klein AM. Scrublet: Computational Identification of Cell Doublets in Single-Cell Transcriptomic Data. *Cell Syst* 2019;8:281–91.
23 Korsunsky I, Millard N, Fan J, *et al*. Fast, sensitive and accurate integration of single-cell data with Harmony. *Nat Methods* 2019;16:1289–96.
24 Trapnell C, Cacchiarelli D, Grimsby J, *et al*. The dynamics and regulators of cell fate decisions are revealed by pseudotemporal ordering of single cells. *Nat Biotechnol* 2014;32:381–6.
25 Hänzelmann S, Castelo R, Guinney J. GSVA: gene set variation analysis for microarray and RNA-seq data. *BMC Bioinformatics* 2013;14:7.
26 Yang W-J, Hao Y-X, Yang X, *et al*. Overexpression of Tie2 is associated with poor prognosis in patients with gastric cancer. *Oncol Lett* 2018;15:8027–33.
27 Luo J, Chen XQ, Li P. The Role of TGF-β and Its Receptors in Gastrointestinal Cancers. *Transl Oncol* 2019;12:475–84.
28 The Cancer Genome Atlas Research Network. Comprehensive molecular characterization of gastric adenocarcinoma. *Nature New Biol* 2014;513:202–9.
29 Bagaev A, Kotlov N, Nomie K, *et al*. Conserved pan-cancer microenvironment subtypes predict response to immunotherapy. *Cancer Cell* 2021;39:845–65.
30 Uwada J, Nakazawa H, Muramatsu I, *et al*. Role of Muscarinic Acetylcholine Receptors in Intestinal Epithelial Homeostasis: Insights for the Treatment of Inflammatory Bowel Disease. *Int J Mol Sci* 2023;24:6508.
31 Ivanov AI, Nusrat A, Parkos CA. Endocytosis of epithelial apical junctional proteins by a clathrin-mediated pathway into a unique storage compartment. *Mol Biol Cell* 2004;15:176–88.
32 Citi S. The mechanobiology of tight junctions. *Biophys Rev* 2019;11:783–93.
33 Jerby-Arnon L, Shah P, Cuoco MS, *et al*. A Cancer Cell Program Promotes T Cell Exclusion and Resistance to Checkpoint Blockade. *Cell* 2018;175:984–97.
34 Jeethy Ram T, Lekshmi A, Darvin P, *et al*. Co-expression of galectin-3 and vimentin in triple negative breast cancer cells promotes tumor progression, metastasis and survival. *Tumour Biol* 2023;45:31–54.
35 Mariño KV, Cagnoni AJ, Croci DO, *et al*. Targeting galectin-driven regulatory circuits in cancer and fibrosis. *Nat Rev Drug Discov* 2023;22:295–316.
36 Matsuishi A, Nakajima S, Saito M, *et al*. The impact of CLDN18.2 expression on effector cells mediating antibody-dependent cellular cytotoxicity in gastric cancer. *Sci Rep* 2024;14:17916.
37 Gao J, Wang Z, Jiang W, *et al*. CLDN18.2 and 4-1BB bispecific antibody givastomig exerts antitumor activity through CLDN18.2-expressing tumor-directed T-cell activation. *J Immunother Cancer* 2023;11:e006704.
38 Chen C, Zhao S, Karnad A, *et al*. The biology and role of CD44 in cancer progression: therapeutic implications. *J Hematol Oncol* 2018;11:64.
39 Hou W, Kong L, Hou Z, *et al*. CD44 is a prognostic biomarker and correlated with immune infiltrates in gastric cancer. *BMC Med Genomics* 2022;15:225.
40 Jia K, Chen Y, Sun Y, *et al*. Multiplex immunohistochemistry defines the tumor immune microenvironment and immunotherapeutic outcome in CLDN18.2-positive gastric cancer. *BMC Med* 2022;20:223.
41 Li J, Zhang Y, Hu D, *et al*. Analysis of the expression and genetic alteration of CLDN18 in gastric cancer. *Aging (Milano)* 2020;12:14271–84.
42 Moran D, Maurus D, Rohde C, *et al*. Prevalence of CLDN18.2, HER2 and PD-L1 in gastric cancer samples. *Ann Oncol* 2018;29:viii32.
43 Kubota Y, Kawazoe A, Mishima S, *et al*. Comprehensive clinical and molecular characterization of claudin 18.2 expression in advanced gastric or gastroesophageal junction cancer. *ESMO Open* 2023;8:100762.
44 Kayikcioglu E, Yüceer RO, Cetin B, *et al*. Prognostic value of claudin 18.2 expression in gastric adenocarcinoma. *World J Gastrointest Oncol* 2023;15:343–51.
45 Arnold A, Daum S, von Winterfeld M, *et al*. Prognostic impact of Claudin 18.2 in gastric and esophageal adenocarcinomas. *Clin Transl Oncol* 2020;22:2357–63.